Hindawi
Advances in Meteorology
Volume 2018, Article ID 9362041, 11 pages
https://doi.org/10.1155/2018/9362041

Research Article

The Use of SPEI and TVDI to Assess Temporal-Spatial Variations in Drought Conditions in the Middle and Lower Reaches of the Yangtze River Basin, China

Shaodan Chen,[1,2] Liping Zhang,[1,2] Xin Liu,[1,2] Mengyao Guo,[1,2] and Dunxian She[1,2]

[1]*State Key Laboratory of Water Resources and Hydropower Engineering Science, Wuhan University, Wuhan 430072, China*
[2]*Hubei Provincial Collaborative Innovation Center for Water Resources Security, Wuhan 430072, China*

Correspondence should be addressed to Liping Zhang; zhanglp@whu.edu.cn

Received 4 March 2018; Revised 12 June 2018; Accepted 9 July 2018; Published 29 August 2018

Academic Editor: Budong Qian

Droughts represent the most complex and damaging type of natural disaster, and they have taken place with increased frequency in China in recent years. Values of the standardized precipitation evapotranspiration index (SPEI) calculated using station-based meteorological data collected from 1961 to 2013 in the middle and lower reaches of the Yangtze River Basin (MLRYRB) are used to monitor droughts. In addition, the SPEI is determined for different timescales (1, 3, 6, and 12 months) to characterize dry or wet conditions in this study area. Moreover, remote sensing methods can cover large areas, and multispectral and temporal observations are provided by satellite sensors. The temperature vegetation dryness index (TVDI) is selected to permit assessment of drought conditions. In addition, the correlation between the SPEI and TVDI values is calculated. The results show that the SPEI values over different timescales reflect complex variations in drought conditions and have been well applied in the MLRYRB. Droughts occurred on an annual basis in 1963, 1966, 1971, 1978, 1979, 1986, 2001, 2011, and 2013, particularly 2011. In addition, the regional average drought frequency in the study area during 1961–2013 is 30%, as determined using the SPEI. An analysis of the correlation between the monthly values of the TVDI and the SPEI-3 shows that a negative relationship exists between the SPEI-3 and the TVDI. That is, smaller TVDI values are associated with greater SPEI-3 values and reduced drought conditions, whereas larger TVDI values are associated with smaller SPEI-3 values and enhanced drought conditions. Therefore, this study of the relationship between the SPEI and the TVDI can provide a basis for government to mitigate the effects of drought.

1. Introduction

In the context of global warming, extreme weather and climatological events, such as flood and drought, appear to occur more frequently [1–5]. In particular, droughts represent a recurrent climatic phenomenon on Earth and are considered to be the most complex natural hazard [6–9]; they have a major impact on water resources, agriculture, natural ecosystems, and society [10–13]. According to the American Meteorological Society, droughts can be classified into four major types, specifically meteorological, hydrological, agricultural, and socioeconomic droughts [4, 14]. Meteorological droughts occur due to a lack of precipitation and high evaporation; they occur frequently and typically trigger other types of droughts [15]. Therefore, efficient monitoring of meteorological droughts is necessary because such monitoring is the basis of providing early warnings and performing risk management in the fields of water resources and agricultural production.

Several drought indices that are calculated using station-based meteorological data are widely used for monitoring drought evolution. These indices include the Palmer drought severity index (PDSI), the standardized precipitation index (SPI), and the standardized precipitation evapotranspiration index (SPEI) [16–20]. The PDSI is calculated using a water balance model originally proposed by Palmer [21], and it considers precipitation, the supply of water, and atmospheric evaporative demand in studying wet and dry conditions. However, PDSI has several disadvantages, including the strong influence of calibration period, drawback in

spatial comparability, and subjectivity in relating drought conditions to the index values [22, 23]. Nevertheless, the main disadvantage of PDSI is that it has a fixed temporal scale; thus, it cannot be used to assess types of droughts that operate at different temporal scales. Hence, McKee et al. [18] used the probabilistic precipitation approach to develop the SPI. The obvious advantages of the SPI are that it is easy to calculate, and it operates over multiple scales. Nevertheless, the SPI is calculated using only monthly precipitation data; thus, it largely ignores the mechanisms by which droughts develop. To overcome this problem, Vicente-Serrano et al. [24] proposed the SPEI, which is based on precipitation and temperature data [17, 25–27]. On short timescales, the SPEI is closely related to soil moisture, while at longer timescales, the SPEI can be related to groundwater and reservoir storage [24]. Therefore, it considers both precipitation and temperature data and combines the sensitivity of the PDSI to changes in evaporation demand with the simplicity of calculation and the multitemporal nature of the SPI [23, 28].

Remote sensing methods, which can cover large areas, and multispectral and multitemporal observations made by satellite sensors over various scales provide other indications of drought conditions on regional scales, especially in areas with few meteorological stations. Numerous studies have suggested that a combination of the normalized difference vegetation index (NDVI) and land surface temperature (LST) can reveal information on regional drought conditions [29–33]. Here, the temperature vegetation dryness index (TVDI), which is based on an interpretation of the simplified NDVI-LST space, is employed to assess drought conditions, and moderate resolution imaging spectroradiometer (MODIS) data are also used [34]. MODIS data have many advanced characteristics, including a wide spectral range, high temporal resolution, and low cost [35, 36].

In this study, we aim (1) to monitor and analyze drought conditions over different timescales (1, 3, 6, and 12 months) in the middle and lower reaches of the Yangtze River Basin (MLRYRB) using SPEI values, (2) to evaluate relationships between SPEI and TVDI, and (3) to investigate options for an alternative drought index for spatial analysis. This paper is organized as follows: the data and methods are described in Section 2; Section 3 gives the results; and the discussion and conclusions are described in Section 4.

2. Data and Methods

2.1. Study Area. The Yangtze River is one of the major rivers in China, and it has a length of approximately 6300 km and a catchment area of approximately 1.8 million km^2. The study area is located in the middle and lower reaches of the Yangtze River (Figure 1(a)). This study area is divided into six subbasins: the Hanjiang River system, the Dongting Lake water system, the middle reaches of the main stream, the Poyang Lake system, the lower reaches of the main stream and the delta plain. The climate in this area is warm and wet in summer and cold and dry in winter. The average annual temperature is approximately 14 to 18°C. The annual rainfall is generally approximately 1000 to 1400 mm and mainly concentrates during the flooding season (April–September), accounting for 70–80% of the annual precipitation. Therefore, taking effective measures to monitor drought conditions in this area is necessary.

2.2. Data. Monthly climate data collected from 1961 to 2013 are used in this study. These data were obtained from the China Meteorological Data Sharing Service System (http://cdc.nmic.cn/home.do), and they include information on precipitation, mean air temperature, maximum and minimum temperature, mean sunshine duration, wind speed, and humidity. Stations with missing meteorological data in any of the 53 years were rejected, and finally, the data from 64 meteorological stations were selected for use in this study.

Additionally, to evaluate the capability of the SPEI to reveal the spatiotemporal variation of drought, the correlations between the SPEI and TVDI values are further analyzed. The MODIS products utilized in this study were obtained from the Earth Observing System Data Gateway of the United States' National Aeronautics and Space Administration (NASA). In this study, the MOD13A3 data product is used. This data product is provided monthly at a resolution of 1 km as a gridded level 3 image in the sinusoidal projection. Eight-day LST data are obtained from the MODIS level 3 land surface temperature products (MOD11A2) with a resolution of 1 km. In addition, eight-day LST values obtained by masking the cloud pixels in the MOD11A2 data product are composited into monthly data, weighted by the number of days recorded in each month. All of the images are converted to the same coordinate system (in this study, the WGS-84 coordinate system) using the MODIS Reprojection Tool (MRT) provided by the Land Processes Distributed Active Archive Center at NASA.

2.3. Standardized Precipitation Evapotranspiration Index. In this study, the SPEI, which is calculated as the difference between precipitation and potential evapotranspiration (PET), is used to describe the severity of drought conditions [26, 37, 38]. The Thornthwaite and Penman–Monteith approaches are widely applied in the calculation of PET [39, 40]. However, the changes in the potential evaporation estimated using the Penman–Monteith method display better agreement than the Thornthwaite method because the Penman–Monteith approach considers humidity and solar radiation, in addition to wind speed, and these variables may capture the magnitude of evapotranspiration [41, 42]. The semiempirical Penman–Monteith method is based on the principles of energy balance and moisture transport, and it takes both thermal and aerodynamic factors into consideration. It is considered to be among the best physically based formulas in the world. As a result, the PET is calculated using the Penman–Monteith equation in the calculation of the SPEI. The equation is expressed as

$$\mathrm{PET} = \frac{0.408\Delta\left(R_n - G\right) + \gamma\left(900/\left(\mathrm{T} + 273\right)\right)\mathrm{u}_2\left(\mathrm{e}_s - \mathrm{e}_a\right)}{\Delta + \gamma\left(1 + 0.34u_2\right)}, \quad (1)$$

where Δ is the slope of the vapor pressure curve; R_n is the net surface radiation; G is the soil heat flux; γ is the

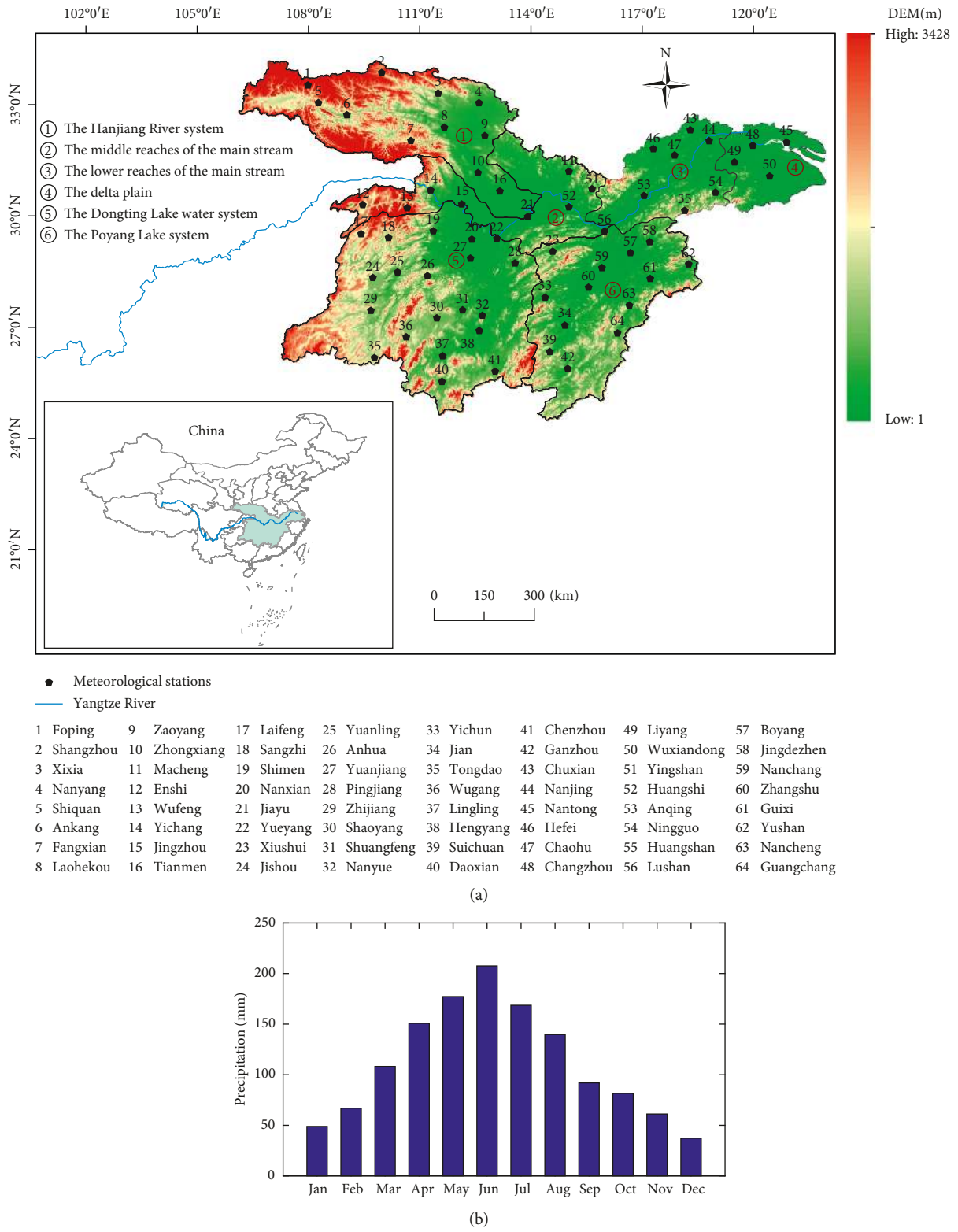

Figure 1: (a) The location of the MLRYRB; (b) monthly mean precipitation averaged over the MLRYRB for the period 1961–2013.

psychrometer constant; u_2 is the wind speed at 2 meters; and e_s and e_a are the saturated vapor pressure at a given air temperature and the actual vapor pressure, respectively.

The SPEI is calculated from the difference between precipitation (P) and PET for month i:

$$D_i = P_i - \mathrm{PET}_i, \tag{2}$$

where D_i is the difference between precipitation and evapotranspiration. The PET is calculated using the Penman–Monteith equation (1).

The calculated D_i values are aggregated over different timescales. In addition, in this work, 1-, 3-, 6-, and 12-month SPEI values are calculated for each station; these quantities are specified as SPEI-1, SPEI-3, SPEI-6, and SPEI-12, respectively.

$$D_n^k = \sum_{i=0}^{k-1} \left(P_{n-i} - \mathrm{PET}_{n-i}\right), \quad n \geq k, \tag{3}$$

where n is the calculation frequency and k is the time scale.

The water balance is then normalized using the log-logistic distribution to calculate the SPEI time series.

$$f(x) = \frac{\beta}{\alpha}\left(\frac{x-\gamma}{\alpha}\right)^{\beta-1}\left[1 + \left(\frac{x-\gamma}{\alpha}\right)^{\beta}\right]^{-2}, \tag{4}$$

where α, β, and γ are scale, shape, and origin parameters, respectively, which can be obtained using the L-moment procedure. The probability distribution function of the D series is then defined as

$$F(x) = \int_0^x f(t)\,dt = \left[1 + \left(\frac{\alpha}{x-\gamma}\right)^{\beta}\right]^{-1}. \tag{5}$$

The SPEI can easily be calculated as the standardized values of $F(x)$ [4, 24].

$$\mathrm{SPEI} = W - \frac{C_0 + C_1 W + C_2 W^2}{1 + d_1 W + d_2 W^2 + d_3 W^3}, \tag{6}$$

where $W = \sqrt{-2\ln(p)}$ and p is the probability of exceeding a determined D value [24]. If $p \leq 0.5$, $p = 1 - F(x)$; if $p > 0.5$, p is replaced by $1 - p$. The constants are $C_0 = 2.515517$; $C_1 = 0.802853$; $C_2 = 0.010328$; $d_1 = 1.432788$; $d_2 = 0.189269$; and $d_3 = 0.001308$. Table 1 shows the drought categories according to the values of the SPEI [18, 43].

2.4. Temperature Vegetation Dryness Index. Remote sensing methods are applied together with station-based meteorological data to determine the temporal and spatial distribution of drought conditions [44, 45]. In this study, the TVDI is used to evaluate the applicability of the SPEI to reveal the spatiotemporal variation of drought and analyze the correlations between the SPEI and TVDI values. Based on remotely sensed observations, the TVDI is defined as

$$\mathrm{TVDI} = \frac{\left(\mathrm{LST} - \mathrm{LST}_{\min}\right)}{\left(\mathrm{LST}_{\max} - \mathrm{LST}_{\min}\right)}, \tag{7}$$

where LST is the observed LST; $\mathrm{LST}_{\max}$ is the maximum temperature in a triangle in the LST-NDVI space and is known as the dry edge, which means the minimum surface water content for the same degree of vegetation coverage; and $\mathrm{LST}_{\min}$ is the minimum temperature (wet edge), meaning that the amount of surface water is sufficient. The $\mathrm{LST}_{\max}$ and $\mathrm{LST}_{\min}$ values are determined by fitting maximum and minimum temperature lines to the NDVI values [46]. Both the wet and dry edges that make up the NDVI-LST triangle represent the results of linear regressions. The resulting equations are represented as:

Table 1: Drought classification based on SPEI values.

Drought categories	SPEI
Nondrought	≥−0.5
Mild drought	(−1.0, −0.5)
Moderate drought	(−1.5, −1.0]
Severe drought	(−2.0, −1.5]
Extreme drought	≤−2.0

$$\begin{aligned} \mathrm{LST}_{\min} &= a_1 + b_1 * \mathrm{NDVI}, \\ \mathrm{LST}_{\max} &= a_2 + b_2 * \mathrm{NDVI}, \end{aligned} \tag{8}$$

where a_1 and a_2 are the intercepts for the wet and dry edges and b_1 and b_1 are the slopes for the wet and dry edges, respectively [41]. Thus, the TVDI can be expressed as

$$\mathrm{TVDI} = \frac{\left[\mathrm{LST} - \left(a_1 + b_1 * \mathrm{NDVI}\right)\right]}{\left[\left(a_2 + b_2 * \mathrm{NDVI}\right) - \left(a_1 + b_1 * \mathrm{NDVI}\right)\right]}. \tag{9}$$

Therefore, to perform further analyses of the efficiency of the SPEI, the TVDI values corresponding to the locations of different meteorological stations are extracted in this study.

3. Results

3.1. Temporal Variations in Drought Conditions. The values of the SPEI calculated over different timescales are beneficial in monitoring drought conditions. According to the methodology described above, the SPEI values of 64 stations calculated for 1961–2013 are averaged to assess dry or wet conditions in the whole MLRYRB, and the regional SPEI is obtained over different timescales (1, 3, 6, and 12 months) using monthly meteorological station-based data for 1961–2013. The SPEI values calculated over different timescales reflect the evolution of wet and dry conditions in different regions of the MLRYRB. Figure 2 shows that the values of the SPEI-1 fluctuates about the zero scale line, reflecting alternating dry-wet conditions throughout 1961–2013 in the MLRYRB. The SPEI-3 shows the characteristics of short-term drought and demonstrates the seasonal variability of drought conditions, which display a greater frequency of fluctuations similar to those seen in the SPEI-1 values. Similarly, the SPEI-6 and SPEI-12 values display the long-term characteristics of drought variability clearly. The results show that the SPEI values over different timescales reflect complex variations in drought conditions.

To illustrate the distribution of drought events in different years, monthly contours are generated. The drought events during 1961–2013 were then superimposed on the monthly contours. Moreover, the SPEI values on a 3-month scale refer to the seasonal water deficits caused by droughts. The SPEI value corresponding to December in each year represents the annual SPEI. Similarly, the May, August, November, and February SPEI values represent the spring, summer, autumn, and winter values, respectively. As shown in Figure 3, mild droughts occur most frequently, followed by moderate droughts. Moreover, the SPEI-1 and SPEI-3 values reflect short-term droughts, whereas the SPEI-6 and SPEI-12 values reflect long-term droughts. In addition,

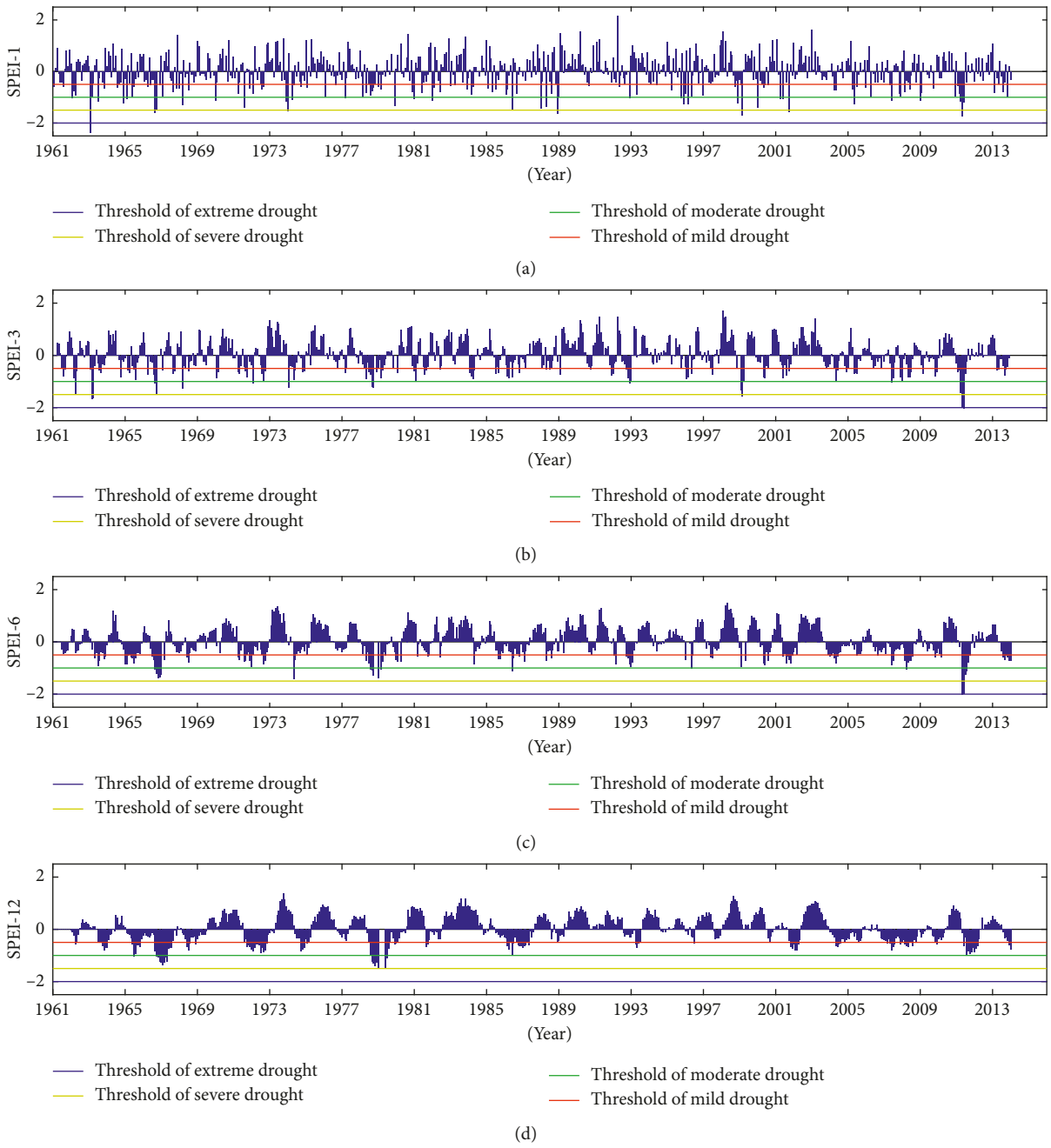

Figure 2: The temporal variability of the SPEI at (a) 1-month lag, (b) 3-month lag, (c) 6-month lag, and (d) 12-month lag.

droughts occurred on an annual basis in 1963, 1966, 1971, 1978, 1979, 1986, 2001, 2011, and 2013. The drought events occurred in the dry year have also been reported by some previous studies [47, 48], which also proves the efficiency of the SPEI in capturing the drought events in our study area.

3.2. Spatial Variations in Drought Conditions. To demonstrate further the spatial and temporal distribution of drought conditions in the study area, the distribution characteristics of drought frequency at the 64 weather stations are analyzed. Using the 53-year records from the weather stations, different levels of drought frequency are computed. Figure 4 shows the drought frequency at the 64 meteorological stations in the MLRYRB based on the SPEI-3 values. These results indicate that mild droughts occur most frequently, followed by moderate droughts; severe and extreme droughts occur relatively infrequently. The regional average drought frequency in the study area during 1961–2013 is 30%, as determined using the SPEI. Daoxian displays the maximum drought frequency, which exceeds 34%; the drought frequencies in Nanjing of Jiangsu province and Jingzhou of Hubei province (33.91% and 33.83%, resp.) are only slightly lower. In addition, Zhijiang

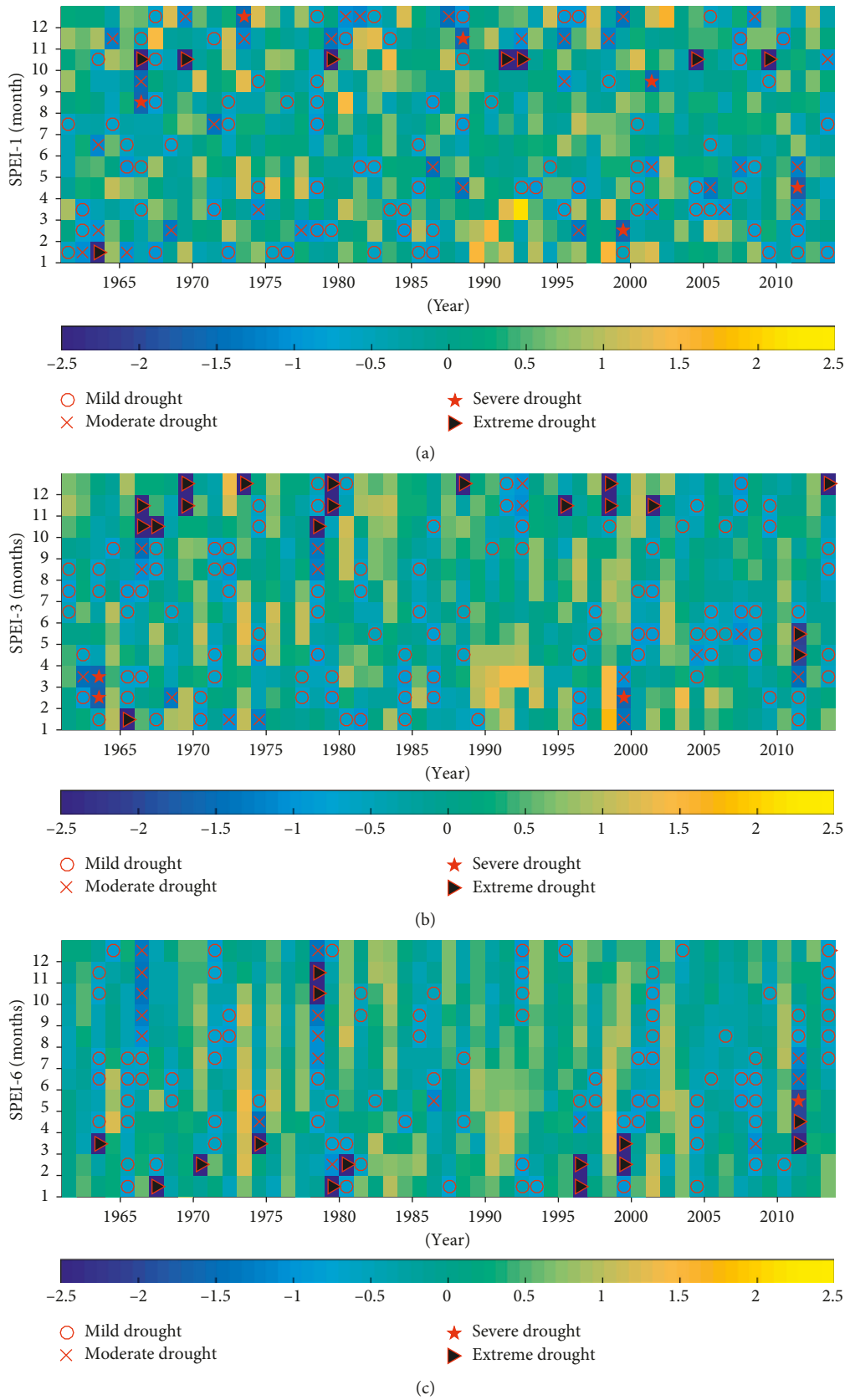

Figure 3: Continued.

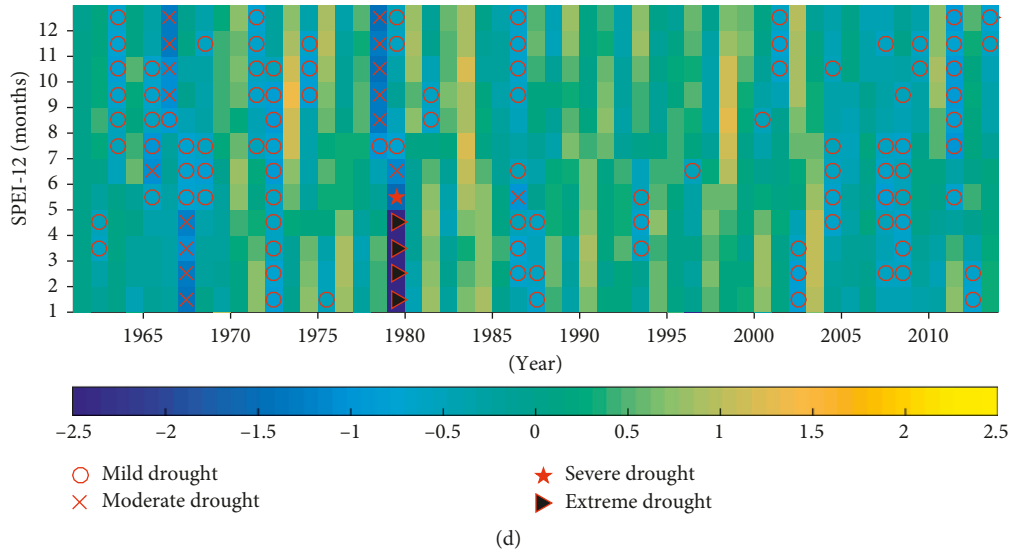

Figure 3: Monthly contours of the (a) SPEI-1, (b) SPEI-3, (c) SPEI-6, and (d) SPEI-12 values and the drought events of different severity grades during 1961–2013. *Note.* SPEI-1, SPEI-3, SPEI-6, and SPEI-12 represent the SPEI values calculated on timescales of 1, 3, 6, and 12 months.

displays the minimum drought frequency of approximately 28%.

3.3. Correlation Analysis between the SPEI and TVDI Values. An analysis of the correlation between the SPEI and TVDI values is evaluated, in which the TVDI values are estimated using scatterplots of LST and NDVI values. A correlation analysis is then conducted between the SPEI and TVDI values, in which the TVDI values are estimated using scatterplots of LST and NDVI values. In this study, the NDVI values are obtained from the MOD13A3 data, and the monthly LST data are obtained from the 8-day MOD11A2 product by taking monthly weighted averages. Table 2 shows the average correlations between the SPEI-3 and TVDI values for all stations in 2013. This table shows that the SPEI-3 and TVDI values are negatively correlated. That is, smaller TVDI values are associated with greater SPEI-3 values and reduced drought conditions, whereas larger TVDI values are associated with smaller SPEI-3 values and enhanced drought conditions. The average correlation between the SPEI-3 and TVDI values in 2013 is −0.58. In addition, the correlation coefficients pass a significance test ($P < 0.05$).

Figure 5 shows the spatial-temporal variability in the distribution of drought conditions detected using the TVDI from January to December in 2013. In these results, the TVDI values range from 0 to 1; lower TVDI values are associated with wetter areas, whereas higher values represent drier areas. On the whole, the northwestern part of the MLRYRB is relatively humid. In addition, the frequency of drought occurrence is high in the central and southeastern parts. The results show that the highest correlation is obtained between the SPEI and TVDI values, which represents a new insight that can be employed in further studies of the combination of meteorological drought indices and remote sensing-based drought monitoring. Previous studies analyzed the relationship between SPEI and remote sensing drought indices [4, 28, 49]. The focus of their research is mainly on the NDVI-derived drought indices, such as the Vegetation Condition Index (VCI). However, NDVI is often referred to a greenness index rather than a drought index [50]. The LST has been found to provide valuable information on surface moisture conditions [51]. Therefore, the analysis of correlations between SPEI and TVDI in this study provides new ideas for monitoring drought.

4. Conclusions

In this study, the temporal and spatial variations in drought conditions over different timescales (1-, 3-, 6-, and 12-month) in the MLRYRB are quantitatively detected and analyzed using the SPEI; meteorological data collected at 64 meteorological stations from 1961 to 2013 are used. Moreover, the spatial distribution of drought conditions is further analyzed using the TVDI, and the correlation between the SPEI and TVDI values is assessed to investigate the efficiency of the SPEI. The main conclusions can be summarized as follows:

(1) The SPEI values over different timescales reflect complex variations in drought conditions and have been well applied in the MLRYRB. Moreover, the SPEI-1 values clearly reflect subtle changes in drought occurrence and reflect short-term conditions, whereas the SPEI-3 values reflect the occurrence of seasonal droughts. Meanwhile, the SPEI-6 and SPEI-12 values indicate long-term variations. Furthermore, Daoxian displays the maximum drought frequency, which exceeds 34%; the drought frequencies in Nanjing of Jiangsu province and Jingzhou of Hubei province (33.91% and 33.83%, resp.) are only slightly lower. In addition, Zhijiang

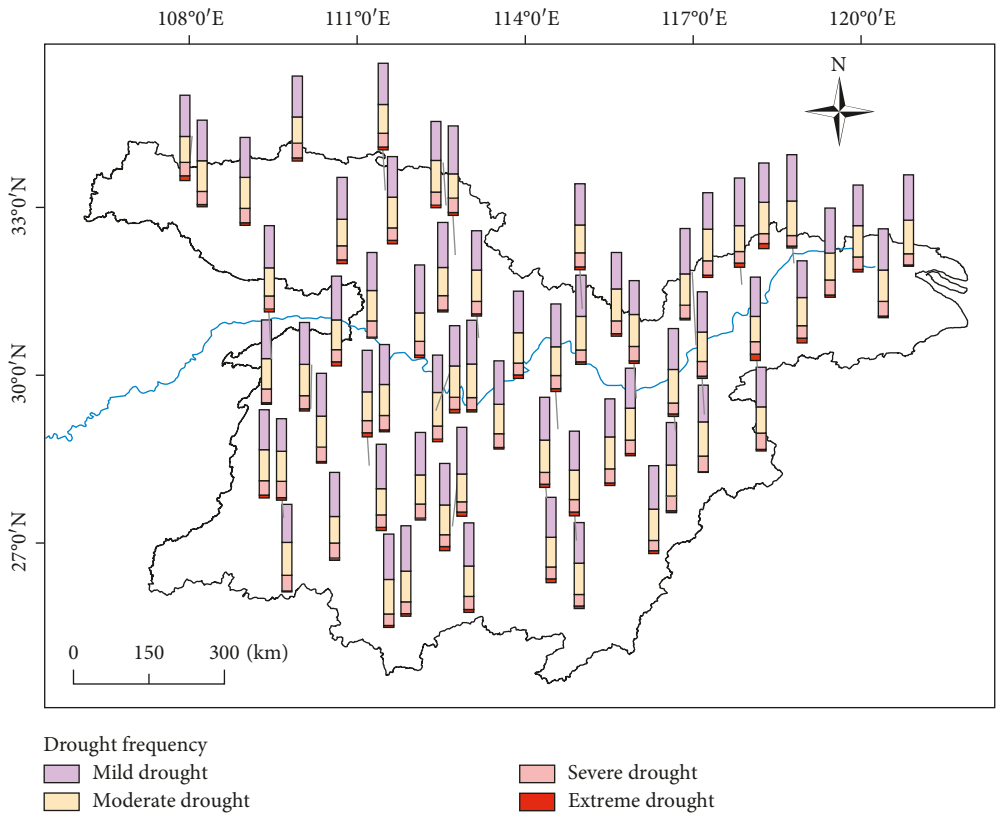

Figure 4: Drought frequency at the 64 meteorological stations in the MLRYRB, as determined using the SPEI-3 values.

Table 2: The average correlations between the TVDI and SPEI-3 values at the stations obtained in each month in 2013.

Month	Correlation	Month	Correlation
Jan.	−0.62	Jul.	−0.49
Feb.	−0.56	Aug.	−0.68
Mar.	−0.47	Sep.	−0.70
Apr.	−0.73	Oct.	−0.55
May	−0.57	Nov.	−0.61
Jun.	−0.54	Dec.	−0.48

displays the minimum drought frequency of approximately 28%.

(2) Strong correlations exist between the SPEI-3 and TVDI values, suggesting that smaller TVDI values are associated with greater SPEI-3 values and reduced drought conditions, whereas larger TVDI values are associated with smaller SPEI-3 values and enhanced drought conditions.

(3) Our study on the relationship between the SPEI and the TVDI can provide a comprehensive analysis of the drought characteristics in the MLRYRB. Therefore, TVDI can be used as an alternative drought index for spatial analysis.

The efficiency of the SPEI in demonstrating changes in dry and wet conditions in the MLRYRB has been well demonstrated [52]. In addition, meteorological droughts normally precede and trigger other types of droughts [4]. In our study, the same standard is used to classify drought conditions based on the SPEI values over different timescales. However, for the same level of agricultural drought, the SPEI threshold values should differ with the time scale, and these threshold values must be confirmed and verified using actual drought conditions. Due to the buffering influence of soil moisture, the values for short timescales should be higher than the values for long timescales. Therefore, comprehensive drought classification over different timescales should be considered in future studies.

In this work, we use a combination of the SPEI and TVDI methods to reconstruct drought conditions in the MLRYRB because this approach reflects changes in drought conditions over multiple scales and considers precipitation and temperature data. This method yields good results in the MLRYRB [53]; however, it has not been compared with other drought indices, such as the SPI and the PDSI [43, 54]. Therefore, future studies will include a comparative analysis of several drought indices. Although many factors are considered by the SPEI method, droughts are affected by topography and human activities, which have considerable effects on the development of droughts. Therefore, future research will focus on how to correctly understand the mechanisms that underlie the observed spatiotemporal differences in drought conditions and how to predict and address the occurrence of droughts, thus supporting the sustainable development of human beings and society.

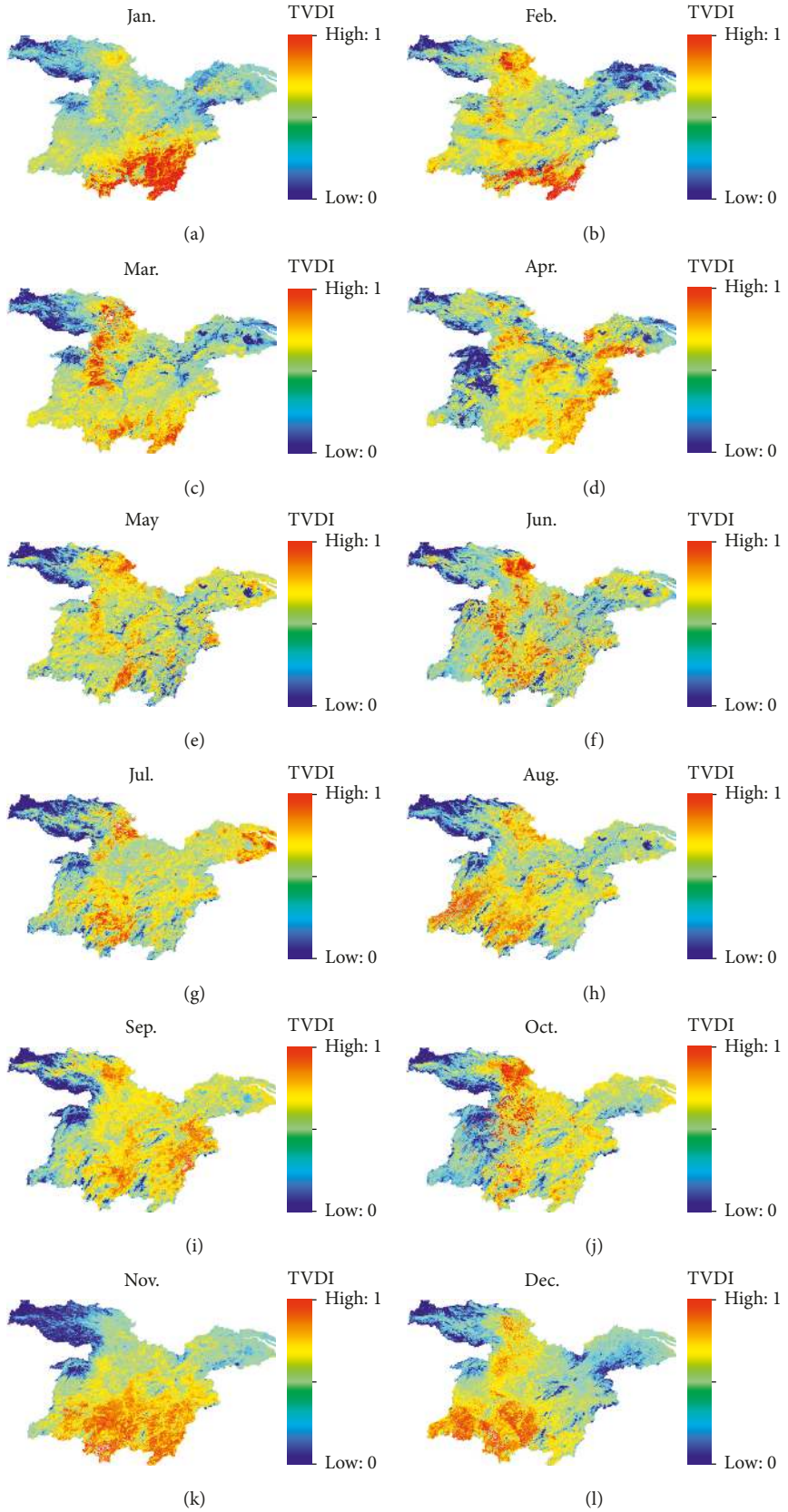

Figure 5: Distribution of drought conditions in the MLRYRB as assessed using the TVDI from January to December in 2013. (a) Jan. (b) Feb. (c) Mar. (d) Apr. (e) May. (f) Jun. (g) Jul. (h) Aug. (i) Sep. (j) Oct. (k) Nov. (l) Dec.

Data Availability

Monthly climate data collected from 1961 to 2013 were obtained from the National Climatic Centre of China Meteorological Administration (http://cdc.nmic.cn/home.do). And the MODIS products utilized in this study were obtained from the Earth Observing System Data Gateway of the United States' National Aeronautics and Space Administration (NASA) (https://earthdata.nasa.gov/).

Conflicts of Interest

The authors declare that they have no conflicts of interest.

Acknowledgments

This study was supported by the National Natural Science Foundation of China (No. 51339004) and the National Key Research and Development Program of China (No. 2017YFA0603704). The authors thank the Earth Observing System Data Gateway of the United States' National Aeronautics and Space Administration (NASA) (https://earthdata.nasa.gov/) for offering the MODIS data. The meteorological data used in this study were collected from the National Climatic Centre of China Meteorological Administration (available on http://cdc.nmic.cn/home.do), which was highly appreciated.

References

[1] C. Gao, H. Chen, S. Sun et al., "A potential predictor of multi-season droughts in Southwest China: soil moisture and its memory," *Natural Hazards*, vol. 91, no. 2, pp. 553–566, 2018.

[2] L. Labudová, M. Labuda, and J. Takáč, "Comparison of SPI and SPEI applicability for drought impact assessment on crop production in the Danubian Lowland and the East Slovakian Lowland," *Theoretical and Applied Climatology*, vol. 128, no. 1-2, pp. 491–506, 2017.

[3] B. Li, Z. Liang, J. Zhang, and G. Wang, "A revised drought index based on precipitation and pan evaporation," *International Journal of Climatology*, vol. 37, no. 2, pp. 793–801, 2017.

[4] X. Li, B. He, X. Quan, Z. Liao, and X. Bai, "Use of the standardized precipitation evapotranspiration index (SPEI) to characterize the drying trend in southwest China from 1982–2012," *Remote Sensing*, vol. 7, no. 8, pp. 10917–10937, 2015.

[5] M. Yu, Q. Li, M. J. Hayes, M. D. Svoboda, and R. R. Heim, "Are droughts becoming more frequent or severe in China based on the standardized precipitation evapotranspiration index: 1951-2010?," *International Journal of Climatology*, vol. 34, no. 3, pp. 545–558, 2014.

[6] L. Tian, S. Yuan, and S. M. Quiring, "Evaluation of six indices for monitoring agricultural drought in the south-central United States," *Agricultural and Forest Meteorology*, vol. 249, pp. 107–119, 2018.

[7] T. Tornros and L. Menzel, "Addressing drought conditions under current and future climates in the Jordan river region," *Hydrology and Earth System Sciences*, vol. 18, no. 1, pp. 305–318, 2014.

[8] T. Sternberg, "Regional drought has a global impact," *Nature*, vol. 472, no. 7342, p. 169, 2011.

[9] M.-J. Yang, D.-H. Yan, Y.-D. Yu, and Z.-Y. Yang, "SPEI-based spatiotemporal analysis of drought in Haihe River Basin from 1961 to 2010," *Advances in Meteorology*, vol. 2016, Article ID 7658015, 10 pages, 2016.

[10] X. G. Xin, R. C. Yu, T. J. Zhou, and B. Wang, "Drought in late spring of South China in recent decades," *Journal of Climate*, vol. 19, no. 13, pp. 3197–3206, 2006.

[11] X. K. Zou, P. M. Zhai, and Q. Zhang, "Variations in droughts over China: 1951–2003," *Geophysical Research Letters*, vol. 32, no. 4, 2005.

[12] E. Lu, Y. L. Luo, R. H. Zhang, Q. X. Wu, and L. P. Liu, "Regional atmospheric anomalies responsible for the 2009-2010 severe drought in China," *Journal of Geophysical Research-Atmospheres*, vol. 116, 2011.

[13] K. Xu, D. Yang, H. Yang, Z. Li, Y. Qin, and Y. Shen, "Spatio-temporal variation of drought in China during 1961–2012: a climatic perspective," *Journal of Hydrology*, vol. 526, pp. 253–264, 2015.

[14] Y. Wang, J. Zhang, E. Guo, Z. Dong, and L. Quan, "Estimation of variability characteristics of regional drought during 1964–2013 in Horqin Sandy Land, China," *Water*, vol. 8, no. 11, p. 543, 2016.

[15] A. K. Mishra and V. P. Singh, "Drought modeling–a review," *Journal of Hydrology*, vol. 403, no. 1-2, pp. 157–175, 2011.

[16] A. Dai, K. E. Trenberth, and T. Qian, "A global data set of palmer drought severity index for 1870–2002: relationship with soil moisture and effects of surface warming," *Journal of Hydrometeorology*, vol. 5, no. 6, pp. 1117–1130, 2004.

[17] S. M. Vicente-Serrano, S. Beguería, J. Lorenzo-Lacruz et al., "Performance of drought indices for ecological, agricultural, and hydrological applications," *Earth Interactions*, vol. 16, no. 10, pp. 1–27, 2012.

[18] T. B. Mckee, N. J. Doesken, and J. Kleist, "The relationship of drought frequency and duration of time scales," in *8th Conference on Apllied Climatology*, American Meteorological Society, Anaheim, CA, USA, January 1993.

[19] R. Brazdil, M. Trnka, P. Dobrovolny, K. Chroma, P. Hlavinka, and Z. Zalud, "Variability of droughts in the Czech Republic, 1881–2006," *Theoretical and Applied Climatology*, vol. 97, no. 3-4, pp. 297–315, 2009.

[20] P. Maca and P. Pech, "Forecasting SPEI and SPI drought indices using the integrated artificial neural networks," *Computational Intelligence and Neuroscience*, vol. 2016, Article ID 3868519, 17 pages, 2016.

[21] W. Palmer, *Meteorological Drought*, US Department of Commerce Weather Bureau Research Paper, Washington, DC, USA, 1965.

[22] W. M. Alley, "The palmer drought severity index: limitations and assumptions," *Journal of climate and applied meteorology*, vol. 23, no. 7, pp. 1100–1109, 1984.

[23] H. Chen and J. Sun, "Changes in drought characteristics over China using the standardized precipitation evapotranspiration index," *Journal of Climate*, vol. 28, no. 13, pp. 5430–5447, 2015.

[24] S. M. Vicente-Serrano, S. Beguería, and J. I. López-Moreno, "A multiscalar drought index sensitive to global warming: the standardized precipitation evapotranspiration index," *Journal of Climate*, vol. 23, no. 7, pp. 1696–1718, 2010.

[25] A. K. Mishra and V. P. Singh, "A review of drought concepts," *Journal of Hydrology*, vol. 391, no. 1-2, pp. 204–216, 2010.

[26] S.-H. Lee, S.-H. Yoo, J.-Y. Choi, and S. Bae, "Assessment of the impact of climate change on drought characteristics in the Hwanghae Plain, North Korea using time series SPI and SPEI: 1981–2100," *Water*, vol. 9, no. 8, p. 579, 2017.

[27] B. Wagan, Z. Zhang, F. Baoping, S. Han, and A. T. Kabo-bah, "Drought trends and temperature influence in Zhanghe River Basin, China," *Advances in Meteorology*, vol. 2015, Article ID 160953, 9 pages, 2015.

[28] Z. Li, T. Zhou, X. Zhao et al., "Assessments of drought impacts on vegetation in China with the optimal time scales of the climatic drought index," *International Journal of Environmental Research and Public Health*, vol. 12, no. 7, pp. 7615–7634, 2015.

[29] L. Du, N. Song, K. Liu et al., "Comparison of two simulation methods of the temperature vegetation dryness index (TVDI) for drought monitoring in semi-arid regions of China," *Remote Sensing*, vol. 9, no. 2, p. 177, 2017.

[30] S. Stisen, I. Sandholt, A. Nørgaard, R. Fensholt, and K. H. Jensen, "Combining the triangle method with thermal inertia to estimate regional evapotranspiration—applied to MSG-SEVIRI data in the Senegal river basin," *Remote Sensing of Environment*, vol. 112, no. 3, pp. 1242–1255, 2008.

[31] X. Cao, Y. Feng, and J. Wang, "An improvement of the Ts-NDVI space drought monitoring method and its applications in the Mongolian plateau with MODIS, 2000–2012," *Arabian Journal of Geosciences*, vol. 9, no. 6, 2016.

[32] L. Liang, S.-h. Zhao, Z.-h. Qin et al., "Drought change trend using MODIS TVDI and Its relationship with climate factors in China from 2001 to 2010," *Journal of Integrative Agriculture*, vol. 13, no. 7, pp. 1501–1508, 2014.

[33] P. Rahimzadeh-Bajgiran, K. Omasa, and Y. Shimizu, "Comparative evaluation of the vegetation dryness index (VDI), the temperature vegetation dryness index (TVDI) and the improved TVDI (iTVDI) for water stress detection in semi-arid regions of Iran," *ISPRS Journal of Photogrammetry and Remote Sensing*, vol. 68, pp. 1–12, 2012.

[34] J. Chen, C. Wang, H. Jiang, L. Mao, and Z. Yu, "Estimating soil moisture using temperature–vegetation dryness index (TVDI) in the Huang-Huai-Hai (HHH) Plain," *International Journal of Remote Sensing*, vol. 32, no. 4, pp. 1165–1177, 2011.

[35] Z. Wan, P. Wang, and X. Li, "Using MODIS land surface temperature and normalized difference vegetation index products for monitoring drought in the southern Great Plains, USA," *International Journal of Remote Sensing*, vol. 25, no. 1, pp. 61–72, 2004.

[36] N. T. Son, C. F. Chen, C. R. Chen, L. Y. Chang, and V. Q. Minh, "Monitoring agricultural drought in the lower mekong basin using MODIS NDVI and land surface temperature data," *International Journal of Applied Earth Observation and Geoinformation*, vol. 18, pp. 417–427, 2012.

[37] S. Beguería, S. M. Vicente-Serrano, F. Reig, and B. Latorre, "Standardized precipitation evapotranspiration index (SPEI) revisited: parameter fitting, evapotranspiration models, tools, datasets and drought monitoring," *International Journal of Climatology*, vol. 34, no. 10, pp. 3001–3023, 2014.

[38] X.-c. Ye, Y.-l. Li, X.-h. Li, C.-y. Xu, and Q. Zhang, "Investigation of the variability and implications of meteorological dry/wet conditions in the Poyang Lake catchment, China, during the period 1960–2010," *Advances in Meteorology*, vol. 2015, Article ID 928534, 11 pages, 2015.

[39] C. W. Thornthwaite, "An approach toward a rational classification of climate," *Geographical Review*, vol. 38, no. 1, pp. 55–94, 1948.

[40] R. G. Allen, L. S. Pereira, D. Raes, and M. Smith, "Crop evapotranspiration. Guidelines for computing crop water requirements," *FAO Irrigation and Drainage Paper*, vol. 56, 1998.

[41] H. L. Penman, "Natural evaporation from open water, bare soil and grass," *Proceedings of the Royal Society of London*, vol. 193, no. 1032, p. 120, 1948.

[42] J. L. Monteith, "Evaporation and environment," *Symposia of the Society for Experimental Biology*, vol. 19, no. 19, pp. 205–234, 1965.

[43] C. Tan, J. Yang, and M. Li, "Temporal-spatial variation of drought indicated by SPI and SPEI in Ningxia Hui autonomous region, China," *Atmosphere*, vol. 6, no. 10, pp. 1399–1421, 2015.

[44] D. Y. Chen, J. F. Huang, and T. J. Jackson, "Vegetation water content estimation for corn and soybeans using spectral indices derived from MODIS near- and short-wave infrared bands," *Remote Sensing of Environment*, vol. 98, no. 2-3, pp. 225–236, 2005.

[45] L. Jiang and S. Islam, "Estimation of surface evaporation map over southern Great Plains using remote sensing data," *Water Resources Research*, vol. 37, no. 2, pp. 329–340, 2001.

[46] I. Sandholt, K. Rasmussen, and J. Andersen, "A simple interpretation of the surface temperature/vegetation index space for assessment of surface moisture status," *Remote Sensing of Environment*, vol. 79, no. 2-3, pp. 213–224, 2002.

[47] W. Wang, L. Li, and X. Cai, "Adaptability of modified CI and SPEI over the middle and lower reaches of Yangtze river basin," *Journal of Tropical Meteorology*, vol. 31, no. 3, pp. 403–416, 2015, in Chinese.

[48] L. Shan, L. Zhang, X. Chen, and W. Yang, "Spatio-temporal evolution characteristics of drought-flood abrupt alternation in the middle and lower reaches of the Yangtze River Basin," *Resources and Environment in the Yangtze Basin*, vol. 24, no. 12, pp. 2100–2107, 2015, in Chinese.

[49] Z. Wang, Z. Huang, J. Li, R. Zhong, and W. Huang, "Assessing impacts of meteorological drought on vegetation at catchment scale in China based on SPEI and NDVI," *Transactions of the Chinese Society of Agricultural Engineering*, vol. 32, no. 14, pp. 177–186, 2016, in Chinese.

[50] T. J. Jackson, D. Y. Chen, M. Cosh et al., "Vegetation water content mapping using Landsat data derived normalized difference water index for corn and soybeans," *Remote Sensing of Environment*, vol. 92, no. 4, pp. 475–482, 2004.

[51] G. G. Gutman, "Towards monitoring droughts from space," *Journal of Climate*, vol. 3, no. 2, pp. 282–295, 1990.

[52] R. Jiang, J. Xie, H. He, J. Luo, and J. Zhu, "Use of four drought indices for evaluating drought characteristics under climate change in Shaanxi, China: 1951–2012," *Natural Hazards*, vol. 75, no. 3, pp. 2885–2903, 2015.

[53] J. Rhee, J. Im, and G. J. Carbone, "Monitoring agricultural drought for arid and humid regions using multi-sensor remote sensing data," *Remote Sensing of Environment*, vol. 114, no. 12, pp. 2875–2887, 2010.

[54] M. Zhao, A. Geruo, I. Velicogna, and J. S. Kimball, "A global gridded dataset of GRACE drought severity index for 2002–14: comparison with PDSI and SPEI and a case study of the Australia millennium drought," *Journal of Hydrometeorology*, vol. 18, no. 8, pp. 2117–2129, 2017.